JOURNAL OF VIROLOGY, Aug. 1989, p. 3284–3295
0022-538X/89/083284-12$02.00/0

Vol. 63, No. 8

Genetic Analysis of the Filamentous Bacteriophage Packaging Signal and of the Proteins That Interact with It

MARJORIE RUSSEL* AND PETER MODEL

The Rockefeller University, 1230 York Avenue, New York, New York 10021-6399

Received 3 January 1989/Accepted 11 April 1989

The single-stranded DNA of filamentous phages (f1, fd, M13, Ike) contains a region that can fold into a hairpin structure that serves to earmark the DNA for encapsidation. Second-site suppressor mutants of f1 that can compensate for deletion of this packaging signal have been isolated and characterized. The mutations lie in three genes, two that encode virion proteins located at the end of the particle that is first to emerge from the cell, the end at which the packaging signal is located, and the third in a gene whose product is required for assembly but which is not itself a part of the virion. Analysis of base substitution and deletion mutations in the packaging signal suggests that both structural and sequence elements are important to its proper function.

Morphogenetic or packaging signals (PS) are *cis*-active regions of a viral genome that earmark it for encapsidation; they have been identified for a number of different viruses. For those that encapsidate double-stranded DNA, such as herpesvirus (8) or bacterial viruses like λ, P22, and P1 (see reference 4 for a review), encapsidation initiates at ends of linear DNA, and the PS is a DNA cleavage signal. For viruses that encapsidate single-stranded nucleic acids, the PS seems to participate directly in assembly. A region of dyad symmetry in single-stranded retroviral RNA is required; its location in an intron (28, 33) allows the selective encapsidation of genomic RNA. Its presence in nonretroviral RNA enables these RNAs to be encapsidated when in cells that have been infected by helper virus (1). The single-stranded RNA-containing bacteriophages contain a hairpin region to which their viral coat protein binds both as a translational repressor (11) and to nucleate capsid formation in vivo (24) and in vitro (3a). A specific capsid protein aggregate from tobacco mosaic virus binds selectively to a region of the single-stranded RNA genome to initiate particle formation (55). This region can direct the efficient in vitro encapsidation of other RNA molecules into pseudovirus particles (48). The critical feature of this signal appears to be the sequence of the loop at the apex of a hairpin structure (51, 52). The single-stranded DNA of the filamentous phage (f1, fd, and M13) also contains a region of dyad symmetry that serves as a PS (see below). In this report we describe genetic efforts to define the signal and the proteins that interact with it.

The assembly of filamentous phage is unusual among bacterial viruses in that it takes place at or in the cytoplasmic membrane of infected cells. Before its encapsidation, single-stranded phage DNA is covered by dimers of the phage-encoded DNA-binding protein, which form a rodlike structure that resembles the phage particle. Phages do not accumulate in the cytoplasm; rather, they are continuously extruded through the cell membrane(s) as they are assembled, without causing cell lysis or death. Phage particles have a fixed diameter, but their length is determined by the size of their single-stranded, circular DNA genome (normally 6,407 nucleotides); defective mini phage particles are shorter than normal, whereas those of phage into which extra DNA has been cloned are proportionately longer (see references 29, 30, 34, and 54 for reviews).

Single-stranded phage DNA contains small but specific regions with double-strand-like properties. About 2% of the genome is resistant to digestion by single-strand-specific nucleases and has the spectral properties expected for double-stranded DNA (43). Sequence analysis of these regions of phage DNA (42) showed a number of potential hairpin structures. The most striking of these can be drawn as a hairpin of 32 base pairs interrupted by a small bulge. There is a major DNA polymerase pause site at the base of this hairpin when single-stranded phage DNA is used as the template (21; unpublished results). The unique susceptibility of this region of the genome to cross-linking by psoralen treatment of intact virions demonstrates that the hairpin also exists within the phage particle (22, 46).

Schaller (41) first suggested that this hairpin might function as a PS. This was confirmed by Dotto et al. (9), who showed that plasmids that contain this hairpin and the phage origin of DNA replication produce and efficiently encapsidate single-stranded plasmid DNA (when phage helper functions are provided); when such plasmids lack the hairpin region, the plasmid single strands are poorly encapsidated. This region functions when cloned at a distance from the filamentous phage replication origin but only if inserted in the same orientation as occurs in the phage (9).

The PS is located at an end of the complex between single-stranded DNA and the phage-encoded single-stranded DNA-binding protein (2) that serves as the precursor to the phage particle. Cross-linking studies demonstrated that the PS is located near an end of the phage particle (45), the end of the assembling particle that is first to emerge from the infected cell (25, 53). Thus the PS determines the orientation of DNA within the particle.

It has been suggested that the PS serves as the initiation point for the replacement of the DNA-binding proteins by the virion structural proteins (25, 53). This would predict that some phage protein(s) might exist that recognizes the PS so as to initiate assembly. We have applied a genetic technique to approach this question. Starting with phage in which the PS had been deleted or interrupted by insertion, mutants with improved efficiencies of packaging were isolated. A number of mutations were mapped and sequenced; half were located in phage genes VII and IX, which encode virion proteins located at the same end of the particle as the

* Corresponding author.

TABLE 1. Construction of deletions and insertions in PS region

Mutant type	Large fragment or parent[a]	Small fragment	Deletion size (bp)	Deletion position[b]	Insertion position[b]	Plaque size	Construct name
Deletion	R289	R296	20	5515–5534		Tiny	R380
	R295	R289	24	5491–5514		Normal[c]	R381
	R295	R296	44	5491–5534			
	R296	R229	81	5535–5614		Tiny	R387
	R289	R229	101	5515–5614		Tiny	R388
Insertion[d]	R296				5534	Tiny	R385
	R229				5613	Normal	R403
	R289				5515	Normal	R404

[a] A large fragment for ΔPS mutants, parent for insertion mutants.
[b] See Fig. 1A for diagram of positions.
[c] On K38(pJLB4).
[d] A 68-bp DNA fragment including the mp18 polylinker inserted into the phage *Eco*RI site.

PS, whereas the other half were in gene I, whose product is required for phage morphogenesis but is not part of the virion. Phage containing mutations in these genes promoted assembly of single-stranded plasmid DNAs that lacked a PS into filamentous transducing particles (TP), suggesting that the wild-type proteins may normally interact with the PS.

The nature of the PS was also investigated by constructing altered or artificial PS; the ability of these signals to function indicates that although the double-stranded nature of the PS contributes to its function, additional elements of structure or sequence are involved.

MATERIALS AND METHODS

Phage and bacterial strains. The unique *Eco*RI sites in phages R289, R295, and R296 were introduced into wild-type f1 DNA (after nucleotides 5514, 5490, and 5534, respectively) by inserting the linker d(AATT) into full-length linear molecules isolated after partial digestion with the enzyme *Tha*I (CG↓CG) (J. Boeke, unpublished results). The f1 nucleotides are numbered throughout according to the DNA sequence of Hill and Petersen (18). The construction of R229 (unique *Eco*RI site after nucleotide 5614) (5), R363 (contains a 6.4-kilobase [kb] *Escherichia coli* DNA insert that includes the *trxB* gene) (37), and R382 (contains the IR-1 and *gtrxA* mutations) (35) was described previously. R383 was constructed by oligonucleotide mutagenesis of R382 as described previously (14, 39); it contains a C-to-T mutation at position 5537 that creates a unique *Mlu*I site in the packaging signal region. *Mlu*I^r derivatives of R383 were isolated after digestion with *Mlu*I, treatment with T4 DNA polymerase and all four deoxynucleoside triphosphates, ligation, and digestion with *Mlu*I.

A unique *Xba*I restriction site was introduced at the beginning of gene IV in a number of phage strains by oligonucleotide mutagenesis; the single nucleotide change required to create the site, T_{4254} to A, changes a leucine codon (UUG) to amber (UAG). The first *Xba*I/amber IV mutant phage was isolated on K870 cells (leucine-inserting suppressor). However, it grew best on a tyrosine-inserting derivative of K38, K833; this strain was used for all subsequent work.

Phage with deletions in the PS region (ΔPS) were constructed by ligating purified *Eco*RI-*Cla*I restriction fragments from double-stranded phage DNAs that contained their *Eco*RI site in different positions as described below (Table 1). Phage with insertions in the PS were constructed as follows: *Eco*RI (8-mer) linkers were added to the *Hae*III fragment from M13mp18 that contains the polylinker region. After digestion with *Eco*RI, the 68-base-pair (bp) fragment that included the polylinker region was cloned into the unique *Eco*RI sites of R296, R229, and R289 to create R385, R403, and R404, respectively.

R465 (PS$^+$ IX A30) was constructed by in vitro recombination (*Eco*RI and *Cla*I) between R289 and R380-L1 so as to restore the PS and retain the suppressor mutation. The PS of R385-L1 was restored by removing (with *Eco*RI) the 63-bp insert, creating R466 (PS$^+$ I A96). R427 is R289 with a unique *Xba*I site in gene IV; R429 is the equivalent derivative of R380-L1 (IX A30), and R431 is the equivalent derivative of R388-L3 (I A96). R433, the product of in vitro recombination (*Xba*I and *Bam*HI) between R429 and R431, has the ΔPS of R380 and both the IX A30 and I A96 suppressor mutations. These phage constructs are listed in Table 2.

E. coli K38 (or its derivatives) was the host for all experiments. K38 containing pJLB4, a gene IV-containing plasmid (J. Brissette, unpublished data), was used as the host for phage containing a truncated gene IV. K1091 (K38 *rep-71*) was used to assay TP.

Mapping mutations that compensate for deletions of the PS. The suppressor mutations were mapped by in vitro recombination, by determining which restriction fragments from parental, wild-type phage DNA could restore the tiny-plaque phenotype to a suppressor-containing ΔPS phage. Phage replicative-form DNAs were digested with two restriction enzymes, each of which had a single site, and the purified DNA fragments were ligated in different combinations, in each case maintaining or regenerating the PS deletion or insertion. Initially, DNA from R380-L1 and from one of its PS$^+$ parents, R289, was digested with *Bam*HI and *Cla*I to generate two fragments. Replacement of the smaller fragment from R380-L1 (which contains genes II, V, VII, VIII, and IX and part of III) by the equivalent fragment from R289 regenerated molecules that formed tiny plaques, indicating that the suppressor was located in this interval. The gene VII through IX regions of R380-L1 and 24 other independently isolated suppressor-containing derivatives of ΔPS phage R380, R387, and R388 and insertion phage R385 were sequenced by the dideoxy-chain termination method (40). Twelve isolates had incurred single mutations in gene IX, whereas one had incurred a mutation in gene VII.

The remaining 12 isolates had no mutation in gene VII or IX. One of them (R388-L3) was chosen for further mapping. The suppressor mutation in this variant was located on the larger *Bam*HI-*Cla*I fragment which includes part of gene III,

TABLE 2. Additional phage and plasmids

Phage or plasmid	Parent(s)	Comments
Phage		
R382	f1$^+$	IR-1 *trxA*; interference resistant
R383	R382	*Mlu*I site in PS
R406	R380	R380-L1; PSΔ20 IX A30
R427	R289	PS$^+$ *Xba*I
R429	R380-L1	PS$^-$ (Δ20) IX A30 *Xba*I
R431	R388-L3	PS$^-$ (Δ101) I A96 *Xba*I
R433	R429, R431	PS$^-$ (Δ20) *Xba*I IX A30 I A96
R465	R289, R380-L1	PS$^+$ IX A30
R466	R385-L1	PS$^+$ I A96
R472	R387	R387-L2; PS$^-$ (Δ81) I A96
R476	R387	R387-L1; PS$^-$ (Δ81) IX A30
R477	R388	R388-L2; PS$^-$ (Δ101) I A96
Plasmids[a]		
pD6		No PS
pD8		PS from f1$^+$
pD18		Missing 17 nucleotides from lower right side of PS
pPMR30		*Mlu*I site in PS (from R383)
pMR30-Δ11		*Mlu*I^r derivative of pPMR30
pPMR30-Δ17		*Mlu*I^r derivative of pPMR30
pPMR31		Artificial PS; head-to-head dimer of 34-bp fragment of *E. coli* DNA
pPMR38		PS from Ike phage (plus orientation)
pPMR39		PS from Ike phage (minus orientation)
pPMR41		PSΔ20 (from R380-L1)
pPMR48		Combined deletions of pD18, R381, pPMR30-Δ11
pHV33		No PS; no f1 origin of DNA replication
pHV33+PS		PS from f1$^+$; no f1 origin of DNA replication

[a] Also diagrammed in Fig. 7 or 8.

all of genes VI, I, and IV, and the intergenic region, including the deleted PS. To subdivide this region, a unique *Xba*I site was introduced into R388-L3 and R289 by oligonucleotide mutagenesis. Subsequent analysis demonstrated that the mutation was located on a 2,035-bp *Xba*I-*Bam*HI fragment that includes part of gene III and all of genes VI and I. DNA sequence analysis indicated that all 12 isolates had incurred a mutation in gene I. The nucleotide and amino acid changes are shown in Table 3.

Plasmid constructions. Table 2 summarizes the plasmids used in this study. The plasmid pD6 contains the f1 origins of minus- and plus-strand DNA replication cloned in the *Bam*HI site of pBR322; its derivative pD8 contains, in addition, the f1 PS region (the 311-bp *Hae*III F fragment) cloned in the *Eco*RI site in the same orientation with respect to the f1 origin as is found in the phage (defined as the plus orientation) (9). pD6 was used for the following plasmid constructions.

(i) The *Hae*III F fragment of R383 was cloned via *Eco*RI linkers into the *Eco*RI site in the plus orientation, creating pPMR30, which has a unique *Mlu*I site in the PS region; derivatives of pPMR30 in which portions of the PS had been deleted were isolated after treatment of *Mlu*I-digested pPMR30 with nuclease S1 (1 μg of DNA with 8 U of S1 for 30 min at 12°C); T4 DNA polymerase and all four deoxynucleoside triphosphates were added before ligation, and the reaction was redigested with *Mlu*I before transformation. Sequence analysis of several isolates showed that, in addition to loss of the *Mlu*I site, adjoining sequences had been deleted to various extents. These plasmids were saved as pPMR30-Δ11 and -Δ17.

(ii) The *Hae*III F fragment of R380-L1 (ΔPS20) was cloned via *Cla*I linkers into the *Cla*I site in the plus orientation, creating pPMR41.

(iii) The 464-bp *Cla*I fragment that contains the packaging signal region of the filamentous phage Ike was cloned into the *Cla*I site, creating pPMR38 (plus orientation) and pPMR39 (minus orientation).

(iv) A 36-bp *Eco*RI-*Bcl*I fragment of *E. coli* DNA was cloned into the *Eco*RI site; pPMR31, a plasmid that contained two copies of the fragment in inverted orientation, was identified by the presence of a ca. 66-bp *Eco*RI fragment that contained a *Bcl*I cleavage site. DNA sequence analysis with both single-stranded and alkaline-denatured double-stranded DNA templates confirmed the construction.

(v) Complementary synthetic oligonucleotides that combined different functional deletions of the PS were cloned between the *Eco*RI and *Hin*dIII sites of the vector, creating pPMR48. The multiply deleted PS of pPMR48 contains the tip deletion from pPMR30Δ11 and a deletion of the base of the hairpin equivalent to pD18 (10) and R381 (Table 1); it

TABLE 3. Summary of suppressor mutations

Parent	Mutation	Amino acid change	Gene	Isolate no(s).	Allele
R380	A_{1293}→G	Thr-30→Ala	IX	L1, L2	A30
	G_{1282}→T	Arg-26→Leu	IX	L3	L26
R385	A_{1293}→G	Thr-30→Ala	IX	L4	A30
	A_{3481}→G	Thr-96→Ala	I	L1, L2, L3, L5, L6	A96
R387	A_{1293}→G	Thr-30→Ala	IX	L1	A30
	G_{1282}→T	Arg-26→Leu	IX	L3	L26
	A_{1186}→G	Ile-27→Val	VII	L4	V27
	A_{3481}→G	Thr-96→Ala	I	L2, L6, L7, L8	A96
	G_{3768}→T	Glu-191→Asp	I	L5	D191
R388	A_{1293}→G	Thr-30→Ala	IX	L1, L6, L7	A30
	G_{1282}→T	Arg-26→Leu	IX	L4, L5	L26
	C_{1281}→T	Arg-26→Cys	IX	L8	C26
	A_{3481}→G	Thr-96→Ala	I	L2, L3	A96

includes f1 sequences 5515 to 5534 and 5546 to 5559 along with an *Eco*RI (5′) and a *Hin*dIII (3′) site.

The plasmid pHV33+PS was constructed by cloning the *Eco*RI fragment from pD8 that contains the f1 PS region into the *Eco*RI site of pHV33 (49), such that the PS was correctly oriented in the single strands (see Results).

Other methods. Double-stranded DNA was prepared as described previously (36), except that for phage DNA log-phase cells (ca. 5×10^8/ml) were infected at 37°C, chloramphenicol was added to a final concentration of 15 μg/ml after 20 min, and the cultures were harvested 90 min later. Other manipulations of DNA were by standard methods (27). DNA sequence analysis with single- or double-stranded DNA templates was by the dideoxynucleotide-chain termination method (40), except that sequencing of the PS region was performed at 50°C.

Particle stability was measured by incubating phage suspended in 10 mM Tris hydrochloride (pH 7.2)–100 mM NaCl at 75°C and sampling at various times. Particle length was measured by electrophoresing lysate samples (diluted with an equal volume of 8% sucrose–0.74 M Tris glycine [pH 9.5]) on horizontal 1.8% agarose–0.37 M Tris glycine (pH 9.5) gels in 0.37 M Tris glycine (pH 9.5). Electrophoresis in a Bio-Rad Mini-Sub gel tank was carried out at 30 to 40 V for 14 to 18 h. Equal titers of TP were electrophoresed, sample lanes were separated by empty lanes, and the gel was not totally submerged in buffer to prevent contamination between samples. To determine titers of phage or TP, individual gel lanes were excised and cut into 0.5-cm fractions, from which particles were eluted by overnight incubation in 1.5 ml of broth. If the particles were to be visualized, the gel was soaked in 0.2 M NaOH to denature the particles, neutralized with Tris hydrochloride (pH 8), and stained with ethidium bromide.

PS activity was determined by infecting log-phase plasmid-containing K38 at a multiplicity of infection of 40. After 10 min at 37°C, the culture was centrifuged and rinsed to remove unadsorbed phage, diluted 400-fold into fresh medium, and incubated at 37°C for 60 min. Incubation was terminated by heating the lysates at 65°C for 10 min to kill viable cells. In some cases, plate lysates were prepared (by plating 10^6 phage with 0.1 ml of the appropriate bacterial culture and incubating overnight at 37°C). Titers of TP were determined by spreading lysate dilutions with concentrated log-phase K1091 (Amp^s) on antibiotic-free plates and then inserting 0.3 ml of ampicillin (15 mg/ml) under the agar. This procedure allowed a period for the TP to infect and for phenotypic expression. K1091 (*rep-71*) was used because filamentous phage cannot replicate in *rep* strains (13), and their absence made it easier to score Amp^r transductants.

RESULTS

Construction of deletions and insertions in the phage PS. The region that contains the filamentous phage PS is shown in Fig. 1A. Also shown are the locations of the unique *Eco*RI sites present in each of four f1 derivatives (R229, R289, R295, and R296). These phage were used to construct molecules that lacked all or part of the PS. Double-stranded, replicative-form DNA from each phage was digested with *Eco*RI and with *Cla*I (which has a single site in f1), and the separated DNA fragments from different phage were combined to create circular molecules missing 20, 24, 44, 81, or 101 bp between *Eco*RI sites in the PS region (Fig. 1B). These DNAs were transfected into competent cells; the results are summarized in Table 1. Deletions that left the end of the

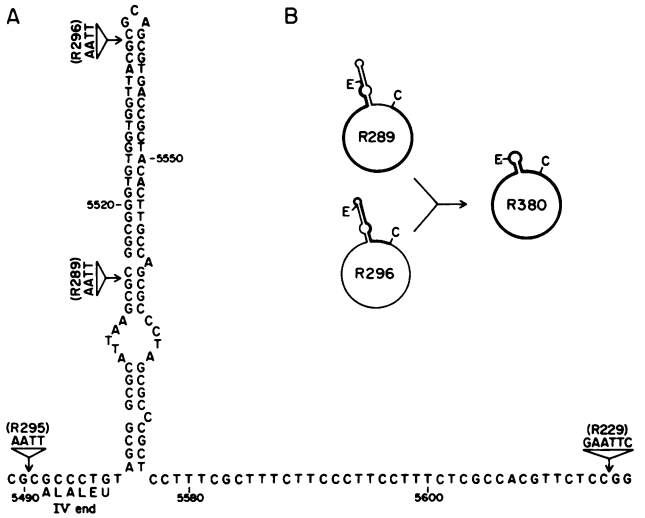

FIG. 1. Location of unique *Eco*RI sites in the PS region and scheme for constructing deletion mutants. (A) The DNA sequence of the PS region of the viral strand of f1 is shown. The names of the f1 derivatives containing an *Eco*RI site, constructed by inserting the linker d(AATT) into *Tha*I sites (Boeke, unpublished results) (i.e., R295, R289, and R296) or into a filled in *Hpa*II site (6) (i.e., R229) at the indicated positions, are also shown. (B) Deletions were constructed by digesting phage double-stranded DNA with *Eco*RI and *Cla*I. In the example shown, the larger fragment of R289 and the smaller fragment of R296 were ligated to create the tiny-plaque-forming phage R380.

gene IV coding region intact (Δ20, Δ81, and Δ101) gave rise to extremely tiny, barely visible plaques. Mutants with one deletion (Δ24), which interrupted the end of gene IV, did not plaque when transfected into the standard f1 host, K38, but made normal-sized plaques when transfected into a strain, K38 (pJLB4), that provides wild-type gene IV protein in *trans*. Mutants with a second construct in which the end of gene IV was interrupted (Δ44) formed plaques in neither host.

Derivatives of R229, R289, and R296 were also constructed in which a 68-bp fragment was inserted into their unique *Eco*RI sites at the positions shown in Fig. 1A (see Materials and Methods). As indicated in Table 1, insertion into R229 or R289 had no effect on plaque size, whereas insertion into R296 created a phage that formed tiny plaques.

Since the PS determines the orientation of DNA within the particle (53), it was possible that its presence is required for particle stability and that formation of tiny plaques is a consequence of particle instability. This was not the case, since the kinetics of thermal inactivation of ΔPS and PS^+ phage were identical (data not shown).

To show that formation of tiny plaques reflected the absence of a functional PS, the ability of a deleted PS to support packaging of a test plasmid was examined. The *Hae*III F fragment of R380-L1 (PSΔ20) (see below), which contains the PS region, was cloned into plasmid pD6, a derivative of pBR322 that contains a functional origin of f1 DNA replication but no PS (9). When pD6-containing cells were infected by an appropriate filamentous helper phage, the phage origin in the plasmid was activated and single-stranded, circular DNA was produced; however, these plasmid single strands were not efficiently packaged into phage-like TP. In contrast, pD8, a derivative of pD6 that does contain a complete PS (the *Hae*III F fragment from $f1^+$ phage cloned in the same orientation as the f1 origin of

replication) is very efficiently packaged (9). The PSΔ20 analog of pD8, pPMR41, was as inefficiently packaged as pD6, about 2% as well as pD8 (see below). Thus a 20-base deletion in the upper portion of the PS hairpin destroys its ability to direct single-stranded DNA into the assembly pathway, and tiny-plaque formation is a reflection of this deficiency.

A number of tiny plaques from each transfection were picked, and titers were determined. They contained fewer phage (6×10^6 to 2×10^7) than normal-sized plaques (3×10^8 to 6×10^8). Furthermore, a variable fraction (10^{-1} to 10^{-4}) of the phage in the tiny plaques formed almost normal-sized plaques. The variants that formed larger plaques bred true, suggesting that revertants or pseudorevertants had been selected.

Isolation and identification of pseudorevertants. A single tiny plaque from each transfection was saved (as R380 [Δ20], R385 [R296+68], R387 [Δ81], and R388 [Δ101]), and a series of independent large-plaque variants was isolated from each (designated R380-L1, -L2, -Ln, etc.). Restriction enzyme analysis of replicative-form DNA of a single variant from each of the deletion phage R380, R387, and R388 showed that a single *Eco*RI site remained and that the size of each deletion was approximately correct. Sequence analysis confirmed the precise extent of each deletion or insertion and demonstrated that no additional sequence changes had occurred within the PS regions. Thus restoration of the ability to form a near-normal-sized plaque (i.e., to produce or assemble phage at closer to normal levels) must be due to compensating mutations located outside the region that contains the PS.

Because of the rapidity with which suppressor mutations arose, quantities of tiny-plaque-forming phage sufficient for genetic or physical analysis could not be prepared. Instead, in vitro recombination was used to map the suppressor mutations in reverse, by determining which restriction fragments from parental, wild-type phage DNA could restore the tiny plaque phenotype to a suppressor-containing ΔPS phage. Phage replicative-form DNAs were digested with two restriction enzymes, each of which had a single site, and the purified DNA fragments were ligated in different combinations, in each case maintaining or regenerating the PS deletion or insertion. In this way, the suppressor mutation in R380-L1 was mapped to a DNA fragment that included genes II, V, VII, VIII, IX, and part of III, quite distinct from the PS itself. Genes VII and IX encode small virion proteins (33 and 32 amino acids long, respectively) located at the same end of the particle as the PS (25), making them good candidates for generating suppressor mutations that compensated for deletion of the PS. Sequence analysis of the gene VII through IX region of R380-L1 revealed a single base substitution, A_{1293} to G, that caused a threonine-to-alanine change at codon 30 in gene IX. This gene IX mutation was named A30. Twenty-five independently isolated suppressor-containing derivatives of ΔPS phage R380, R387, and R388 and insertion phage R385 were sequenced in this region (Table 3). Six additional isolates of the A30 mutation in gene IX were identified. Four phage had incurred a G-to-T change at position 1282, changing codon 26 of gene IX from arginine to leucine, whereas one contained a C-to-T change at position 1281 that changed this same arginine to cysteine. A single isolate had incurred an A-to-G change at position 1186, changing codon 27 of gene VII from isoleucine to valine (V27). This mutation also altered the -10 region of the gene VIII promoter (42) (which encodes the major coat protein), and cells infected by the phage that carried this mutation produced less major coat protein, about 40% as much as wild-type infections (data not shown). Because of the difficulty in determining whether the reduced amount of gene VIII protein or the altered gene VII protein was responsible for the improved growth of the ΔPS phage, and because no other (simpler) gene VII mutations were isolated, this mutant phage was put aside.

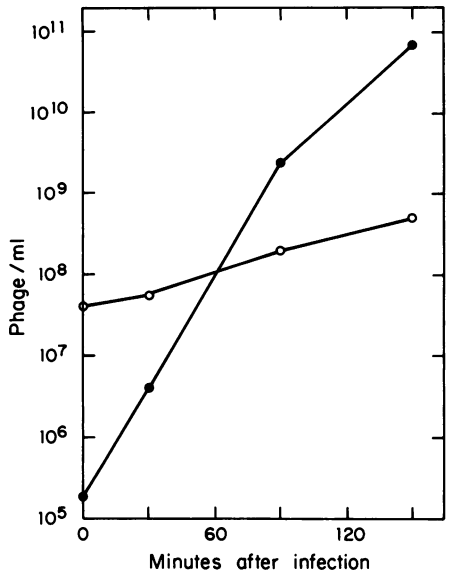

FIG. 2. Rate of production of ΔPS phage. An agar plug containing a single, tiny R380 plaque in 0.5 ml of broth was incubated at 37°C with 0.5 ml of a growing culture (ca. 4×10^8 cells per ml) of bacteria. Samples were withdrawn at the times indicated, heated at 65°C for 5 min to eliminate infective centers, and plated. The numbers of tiny plaques (○) and large plaques (●) were scored for each sampling time.

The remaining 12 isolates had no mutation in gene VII or IX. One of them (R388-L3) was chosen for further mapping. In vitro recombination indicated that the suppressor mutation in this phage was located on a DNA fragment that includes part of gene III and all of genes VI and I. Gene I encodes a protein that is required for filamentous phage assembly but is not part of the virion (genes III and VI encode proteins located at the end of the phage opposite from the PS), making it a good candidate for containing the suppressor mutation. Sequence analysis of the R388-L3 gene I indicated a single A-to-G change at position 3481 that changed codon 96 from threonine to alanine (A96). Eleven of the 12 remaining phage had incurred the identical mutation, whereas the 12th, R387-L5, had incurred a single G-to-T change at position 3768, changing codon 191 from glutamic acid to aspartic acid (D191). A summary of the mutations that compensate for inactivation of the PS is shown in Table 3.

Characterization of phage with PS deletions and compensatory mutations. The low titer of phage in a tiny plaque and the large fraction that have already incurred compensating mutations (10^{-1} to 10^{-4}) reflects how poorly the ΔPS phage that lack a compensating mutation are produced. This is illustrated by the growth curves presented in Fig. 2. A single (tiny) R380 plaque was used to infect an excess of cells, and samples were assayed at the indicated times for the number of tiny-plaque and near-normal-plaque producers. Although the initial fraction of suppressor-containing phage was low (5×10^{-3}), within 60 min it had reached the same level as its

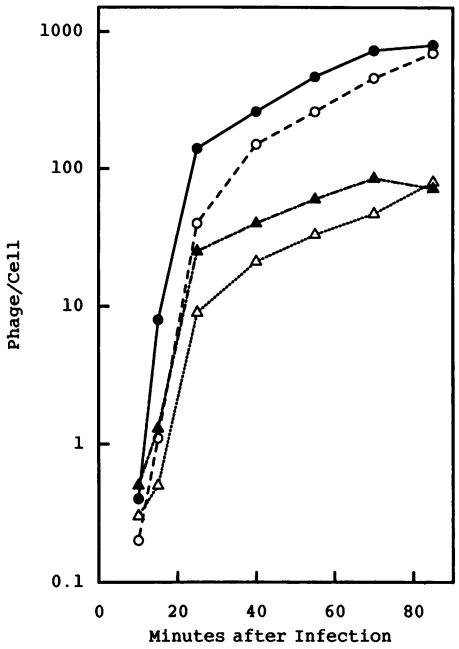

FIG. 3. Rate of production of ΔPS phage containing the I A96, IX A30, or both suppressor mutations. Bacteria (K38 supF) grown at 37°C to 3.5 × 10^8 cells per ml were infected by phage at multiplicities of infection of 80. After 8 min, the cultures were centrifuged, rinsed, suspended, and diluted 10^4-fold. The cultures were assayed for viable cells and infective centers (data not shown; see the text); at the times indicated, samples were removed into $CHCl_3$, and phage titers were determined. Symbols: ●, R427 (PS^+ I^+ IX^+); ▲, R431 (ΔPS I A96 IX^+); △, R429 (ΔPS I^+ IX A30); ○, R433 (ΔPS I A96 IX A30).

tiny-plaque-forming parent. In 150 min of growth, the large-plaque formers increased more than 10^5-fold, whereas the tiny-plaque-forming parent increased 10-fold.

With the kinetics of phage production as an indicator (Fig. 3), compensating mutations in genes IX and I restored ΔPS phage to close-to-normal assembly rates at early times after infection. The decline in their rate of production at later times likely reflected the reduced viability of the cells they infected (5% for the I mutant and 15% for the IX mutant, compared with 50% for the PS^+ control); reduced viability, in turn, implied that the normal balance of DNA and protein synthesis with assembly was not precisely maintained and suggested that the mutant proteins were unable to fully restore the assembly rate to a level that could keep up with the supply of components. Phage production and infected cell survival with R433, a ΔPS phage that contains both the gene IX and gene I suppressor mutations (constructed by in vitro recombination), were very close to those of the PS^+ control, better than either suppressor alone. Thus the effects of the compensating mutations are additive.

Suppressor mutations act in *trans*. Because ΔPS phage accumulated mutations so rapidly, stocks that had not incurred compensating mutations could not be prepared, and characterizations such as those described above necessarily involved comparisons between wild-type and doubly mutant phage (i.e., ΔPS and a compensating mutation). To examine the effects due solely to the compensating mutations, intact PS were restored to a ΔPS-IX A30 and a ΔPS-I A96 phage by reversing the in vitro recombination procedure that had been initially used to construct them. R465 (PS^+ IX A30) and R466 (PS^+ I A96) grew better than their ΔPS parents, forming plaques that were indistinguishable from wild-type phage. R465 and R466 phage supported the formation of filamentous TP from plasmid pD6 (which lacks the f1 PS) at higher efficiencies than did the isogenic control phage, R289 (Table 4). Both the absolute titer of TP and the titer relative to the helper phage yield were stimulated about 10-fold. Thus suppressor mutations in both genes work in *trans*, and the gene IX and I proteins promote morphogenesis of single strands that lack a PS. These suppressors still "recognize" the PS, since R465 and R466 support TP formation from pD8 (pD6+PS) at higher efficiencies than from pD6, in this case at about the same efficiency as R289 (Table 4).

The plasmid pC194 is one of a number of broad-host-range, small plasmids isolated from gram-positive bacteria that is capable of replicating in gram-negative bacteria and exists as both double-stranded and single-stranded DNA in *Bacillus subtilis* (50) and *E. coli* (as a chimera with pBR322, called pHV33), reflecting a rolling-circle mode of replication (17, 49) like that in filamentous phage. The intracellular concentration of single strands is low (49); they represent

TABLE 4. Effect of suppressor mutations on encapsidation of single-stranded plasmid DNA[a]

Helper phage	Plasmid	Phage titer/ml	TP titer/ml	TP/phage ratio
R289 (wild type)	pD6 (PS^-)	9.7×10^{10}	1.6×10^9	0.02
R465 (IX A30)	pD6 (PS^-)	8.4×10^{10}	1.5×10^{10}	0.18
R466 (I A96)	pD6 (PS^-)	7.7×10^{10}	4.0×10^{10}	0.52
R289 (wild type)	pD8 (PS^+)	6.8×10^{11}	1.2×10^{11}	0.18
R465 (IX A30)	pD8 (PS^+)	5.4×10^{11}	1.3×10^{11}	0.24
R466 (I A96)	pD8 (PS^+)	4.3×10^{11}	1.4×10^{11}	0.33
R289 (wild type)	pHV33	4.5×10^{12}	2.8×10^8	6.2×10^{-5}
R465 (IX A30)	pHV33	4.6×10^{12}	4.8×10^7	1.0×10^{-5}
R466 (I A96)	pHV33	5.1×10^{12}	3.5×10^9	6.9×10^{-4}
R476 (ΔPS IX A30)	pHV33	1.9×10^{12}	2.5×10^{10}	1.3×10^{-2}
R472 (ΔPS I A96)	pHV33	4.9×10^{12}	3.4×10^{10}	6.9×10^{-3}
R289 (wild type)	pHV33+PS	3.5×10^{12}	3.0×10^9	8.6×10^{-4}
R465 (IX A30)	pHV33+PS	3.7×10^{12}	2.0×10^9	5.4×10^{-4}
R466 (I A96)	pHV33+PS	5.2×10^{12}	1.8×10^{10}	3.5×10^{-3}

[a] Lysates were prepared by plating 10^6 phage with 0.1 ml of stationary-phase cultures of K38 carrying the indicated plasmid. After overnight incubation at 37°C, the lysates were harvested and titered as described in Materials and Methods.

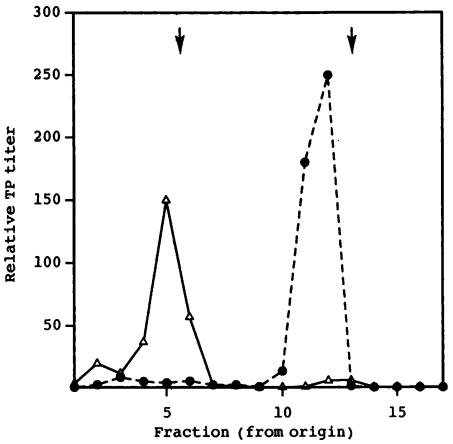

FIG. 4. Size of pHV33 and pHV33+PS TP. TP lysates of pHV33 (Δ) and pHV33+PS (●) prepared with R289 helper phage were electrophoresed and eluted, and titers were determined as described in Materials and Methods. The TP titers were scaled arbitrarily so that the peak portions of particles from lysates with different titers could be displayed on a single plot. The positions of the marker phage peaks (R363, 12.8 kb; R289, 6.4 kb) are indicated by arrows.

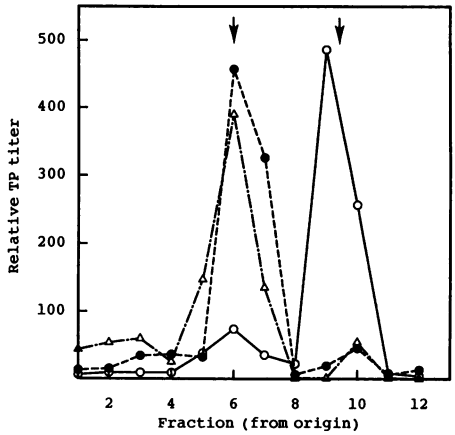

FIG. 5. Effect of gene I or gene IX suppressor mutations on the size of pHV33 TP. TP lysates of pHV33 prepared with R289 (wild type) (Δ), R465 (IX A30) (●), or R466 (I A96) (○) helper phage were electrophoresed on an agarose gel and eluted, and titers were determined as described in Materials and Methods. The positions of the marker phage peaks (R363, 12.8 kb; R289, 6.4 kb) are indicated by arrows.

less than 0.5% of total single strands in an f1-infected, pHV33-containing cell (data not shown). The pHV33 single-stranded DNA can be encapsidated into TP when filamentous helper phage are present (7). These TP, which are longer than expected for the size of the plasmid, contain a plasmid single strand coencapsidated with a helper phage genome (7). Upon disruption of the particles, separate plasmid (7.3-kb) and helper-phage (6.4-kb) single-stranded DNAs are released (B. Michel, personal communication). This suggests that pHV33 single strands cannot initiate encapsidation and that they can only be encapsidated into assembling particles that already include a helper phage genome. A failure to terminate encapsidation after a single phage genome has been incorporated is not uncommon; about 2 to 5% of wild-type phage particles are double length and contain two unit-length genomes (3, 44). Introduction of an f1 PS into pHV33 (as in pHV33+PS, in which the PS is cloned so that its orientation in the plasmid single strand is identical to that in pD8 or phage single strands) leads to a ca. 10-fold increase in the absolute and relative numbers of TP generated (Table 4).

Figure 4 confirms that >99% of the pHV33 TP are coencapsidated and shows that pHV33+PS TP are independently packaged. Lysates containing R289 helper phage and either pHV33 or pHV33+PS TP were electrophoresed on a 1.8% agarose gel at pH 9.5. At this pH the particles, which carry a net negative charge on their solvent-exposed surface, migrate as a function of their length (30). After electrophoresis the gel lanes were sliced, the phage and TP were eluted, and titers were determined. The pHV33 TP migrated slightly more slowly than R363 (a 12.8-kb marker phage), consistent with the length expected for particles that contain one molecule of pHV33 and one of R289 DNA (7.3 + 6.4 = 13.7 kb). The pHV33+PS TP migrated much faster, as would be expected for particles containing a single genome.

To examine the effect of the suppressor mutants on encapsidation of pHV33, lysates were prepared with helper phage that contained a wild-type PS and either a gene I or a gene IX suppressor mutation. The TP yield was 10-fold higher with helper phage that contained the gene I mutation (A96) than with the wild-type control; with helper phage that contained the gene IX mutation (A30) the yield was actually lower (Table 4). Analysis of particle size (Fig. 5) showed that more than 90% of the TP produced with mutant pI were unit length, despite the absence of a PS in the pHV33 genome. By contrast, >95% of those produced with mutant pIX were coencapsidated, like the control.

The situation was different when the helper phage did not contain a PS. Under these circumstances there was an increase in the yield of TP no matter which suppressor was used (Table 4), and most of these TP were singly encapsidated (data not shown). Hence competition from PS-containing helper phage can prevent independent initiation of packaging of DNA molecules which themselves do not contain a PS.

pD6, which like pHV33 lacks a PS, was primarily singly encapsidated into particles that reflected its 5-kb genome; when wild-type (R289) helper phage were used, more than 95% of the pD6 particles were unit length (Fig. 6). This plasmid contains the f1 replication origin, and substantial amounts of single strands are generated when phage replication functions are provided (9). Because the plasmid copy number is high relative to that of the infecting phage, the phage origin on the plasmid is used by the phage replication proteins at the expense of phage templates. This leads to a high concentration of plasmid DNA relative to phage DNA in the infected cell. When an interference-resistant helper is used, the balance of phage and plasmid DNA synthesis is altered, and the ratio of phage to plasmid DNA is increased (12). Under these circumstances, about 30% of the pD6 TP are coencapsidated with helper phage (Fig. 6). Hence the ratio of singly to doubly encapsidated pD6 molecules is related to their concentration relative to that of the helper DNA.

Further definition of the packaging signal. To test whether the sequence at the tip of the PS hairpin is critical for its recognition, a series of phages with minor tip alterations was generated. Preliminary experiments showed that the yields of these mutant phages were normal (data not shown). A more sensitive assay is to test the ability of the altered PS to compete with a wild-type PS. In the experiment presented in

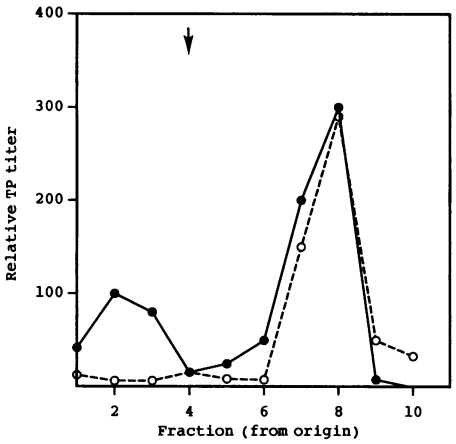

FIG. 6. Size of pD6 TP. TP lysates of pD6, prepared with R289 (○) phage or with the interference-resistant phage, R382 (●), were electrophoresed on an agarose gel and eluted, and titers were determined as described in Materials and Methods. The position of the marker phage peak (R289, 6.4 kb) is indicated by an arrow.

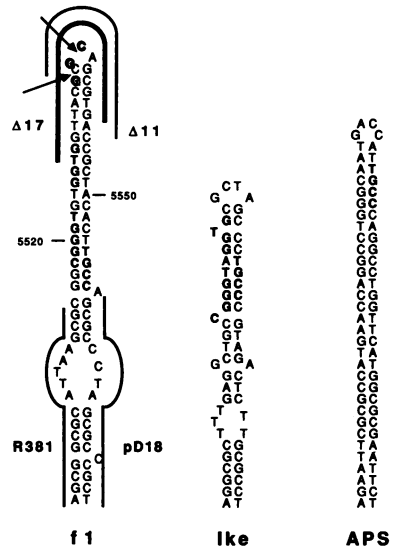

FIG. 7. Comparison of the f1, Ike, and artificial PS. The sequences of the PS region of f1 (18, 42) and Ike (31) are shown in the folded form predicted for the single, genomic strand. The artificial PS (APS) is a head-to-head dimer of an *Eco*RI-*Bcl*I restriction fragment of *E. coli* DNA. The extent of the deletions of the f1 PS carried in R381, pD18, or pPMR30Δ11, all of which do not impair function, are shown by the thinner line. The deletion carried by pPMR30Δ17, which destroys PS function, is shown by the heavier line. The arrows indicate the positions at which up to four nucleotides can be inserted without disrupting function (R296, R383-*Mlu*I^r-2). Insertion of 68 nucleotides at the position of the lower arrow disrupts PS function (R385). Base substitutions at the shadowed nucleotides near the tip have no effect (R383, R383-*Mlu*I^r-6, -8, -9). Nucleotides in boldface type indicate homologies between the Ike PS and the essential region of the f1 PS.

Table 5, the cells carried pD8 (PS$^+$), and the relative yield of TP to phage was measured. When the helper phage contained a defective PS, as in R408, the relative yield of TP increased 10-fold. By contrast, base substitutions or a two-base insertion at the tip of the PS had no such effect. R383 phage (C_{5537}→T, which creates a unique *Mlu*I site) were not more effective in encapsidating pD8 (PS$^+$) than R382, which contains a wild-type PS. Similarly, *Mlu*I-resistant derivatives of R383 in which A or T had replaced G_{5536} in the hairpin loop, in which T replaced G_{5534} adjacent to the loop, or in which GC was inserted after position 5536 in the loop retained full PS activity. Phage R296 (Fig. 1A) formed normal-sized plaques; thus a four-base insertion at the tip did not disrupt PS function either.

Among the original insertion and deletion constructs, two phage, R381 (Δ24) and R404 (+68), formed normal-sized plaques upon transfection into the appropriate strain. The deletion in R381 (from positions 5490 to 5514) removed the lower left portion of the 78-nucleotide PS region (Fig. 7). The insertion in R404 was at the *Eco*RI site of R289, located between bases 5514 and 5515, just above the bulge or region of noncomplementarity. Sequence analysis confirmed that neither R381 nor R404 had incurred suppressor mutations at any of the positions identified for the other deletion or insertion mutant phage. Their normal plaque size and the apparent absence of suppressor mutations suggest that the lower-left-hand portion of the hairpin (including the bulge) is not an essential part of the PS. Given the double-stranded nature of the PS region, this is consistent with the observation of Dotto and Zinder (10) (Table 6) that pD18, a derivative of plasmid pD6 containing a truncated PS region that is missing the lower-right-hand portion of the hairpin beyond nucleotide 5559 (Fig. 7), is as efficiently assembled into TP as pD8, which contains the entire hairpin.

What other features of the hairpin determine its activity as a PS? Table 6 presents the results of an experiment in which cells containing pD6-derived plasmids with altered PS regions were infected with helper phage, and the efficiency of TP formation was determined. Figure 7 is a diagram of some of the altered PS constructs, and Fig. 8 shows their postulated structures. pPMR41, an analog of pD8 in which 20 bases (5515 through 5534) have been deleted (as in the ΔPS20 phage R380), assembled into TP at the same low efficiency as pD6. Thus deletion of the predicted 20 bp that form the upper portion of the hairpin eliminates PS function. pPMR30Δ11, a plasmid in which 11 bases (5535 through 5545) are deleted, retained activity. Loss of six additional bases (5527 through 5543), as in pPMR30Δ17, which should remove an additional 2 bp, eliminated PS activity. Clearly, structure is critical, since the PS in pPMR48, in which both the nonessential regions defined by R381 and pD18 (the base) and by pPMR30Δ11 (the tip) were deleted, was not active (Table 6). Although specific base recognition is not excluded, some structure that can be provided either by the

TABLE 5. Effect of changes at the PS tip[a]

Phage	Change	Position	TP/phage ratio	Normalized ratio[b]
R382			0.14	1
R383(*Mlu*I)	C→T	5537	0.14	1
R383-*Mlu*I^r-2	+GC	5536	0.14	1
R383-*Mlu*I^r-6	G→T	5534	0.14	1
R383-*Mlu*I^r-8	G→A	5536	0.18	1.3
R383-*Mlu*I^r-9	G→T	5536	0.15	1
R408	PSΔ20	5515–5534	1.5	10.7

[a] K38 containing pD8 were grown to an optical density 0.6 and infected by R382 or derivatives of R382 containing the indicated changes in the PS at a multiplicity of infection of 40. After 10 min, the cells were centrifuged, suspended, and diluted 10^4-fold. After incubation at 37°C for 60 min, the samples were heated to 65°C to kill viable cells. Phage and TP were assayed as described in Materials and Methods.

[b] Normalized to the TP/phage ratio obtained with R382.

TABLE 6. Effect of PS alterations on TP formation[a]

Helper	Plasmid	PS	Phage titer/ml	TP titer/ml	TP/phage ratio
PS$^+$	pD6	−	1.9×10^8	2.0×10^6	0.01
PS$^+$	pD8	+	2.1×10^8	1.1×10^8	0.52
PS$^+$	pD18	Δbase	1.4×10^8	6.6×10^7	0.47
PS$^+$	pPMR41	Δ20	1.0×10^8	6.5×10^5	0.007
PS$^+$	pPMR30(Δ11)	Δ11	1.5×10^8	8.8×10^7	0.59
PS$^+$	pPMR30(Δ17)	Δ17	2.5×10^8	2.4×10^6	0.01
PS$^+$	pPMR48	Δ11, base	4.2×10^7	1.3×10^6	0.03
PS$^+$	pPMR31	APS	2.0×10^8	7.2×10^6	0.04
PS$^+$	pPMR38	Ike PS (+)	4.1×10^7	2.8×10^7	0.68
PS$^+$	pPMR39	Ike PS (−)	1.9×10^8	2.0×10^5	0.001
ΔPS IX A30	pD6	−	2.6×10^7	9.8×10^6	0.38
ΔPS IX A30	pD8	+	1.3×10^7	5.0×10^7	3.9
ΔPS IX A30	pPMR30(Δ11)	Δ11	1.3×10^7	1.1×10^8	8.5
ΔPS IX A30	pPMR30(Δ17)	Δ17	1.1×10^7	8.0×10^6	0.72
ΔPS IX A30	pPMR48	Δ11, base	5.0×10^6	7.0×10^5	0.14
ΔPS IX A30	pPMR31	APS	8.0×10^6	3.5×10^7	4.4
ΔPS IX A30	pPMR38	Ike PS (+)	4.0×10^6	6.5×10^7	16.0
ΔPS IX A30	pPMR39	Ike PS (−)	1.3×10^7	1.0×10^6	0.08
ΔPS I A96	pD6	−	2.9×10^7	2.8×10^7	1.0
ΔPS I A96	pD8	+	3.7×10^7	1.5×10^8	4.1
ΔPS I A96	pPMR31	APS	3.6×10^7	1.1×10^8	3.1
ΔPS I A96	pPMR38	Ike PS (+)	6.5×10^6	6.5×10^7	10.0
ΔPS I A96	pPMR39	Ike PS (−)	3.8×10^7	6.5×10^6	0.17

[a] K38 bacteria containing the indicated plasmids were grown in fortified broth containing 100 μg of ampicillin per ml to an optical density 0.6. Phage (R289, PS$^+$; R406, ΔPS IX A30; R477, ΔPS I A96) were added at a multiplicity of infection of 40. After 10 min at 37°C, the cultures were centrifuged, rinsed to remove unadsorbed phage, and diluted 400-fold. After 60 min of incubation, the samples were heated to 65°C to kill viable cells, and titers of the phage and TP were determined as described in Materials and Methods.

bottom or by the top portion of the hairpin must also be present.

The plasmid pPMR31 is a pD6 derivative that contains two copies of a 36-bp restriction fragment (of *E. coli* DNA) inserted in a head-to-head orientation to potentiate hairpin formation. This insertion might act as an artificial PS, with a hairpin longer than the actual PS hairpin (Fig. 7). With wild-type (R289) helper phage, pPMR31 TP were produced at very low efficiency (Table 6), which suggests that a specific base sequence or a structural feature other than simple double strandedness is required for PS activity.

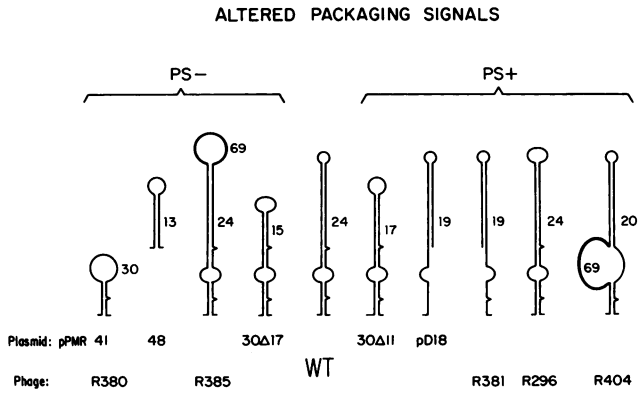

FIG. 8. Proposed structure of the wild-type (WT) and altered PS. A schematic representation of the structure of the f1 PS as originally proposed by Schaller et al. (42) is marked as WT. The other diagrams represent the structures expected for the altered PS. The number at the side of each upper hairpin refers to the predicted number of base pairs remaining in that stem. The numbers near the large loops show the number of unpaired nucleotides expected. PS$^+$ structures function; PS$^-$ structures do not. The names of the phages and/or plasmids that contain these constructs are given at the bottom.

The efficiency of TP formation was also determined by using helper phages (R406 and R477) that themselves lacked a functional PS and had compensating mutations in genes I and IX, respectively (Table 6). Since ΔPS phage that contained a suppressor mutation were assembled somewhat less efficiently than wild-type phage (Fig. 3), and since the suppressor mutations acted in *trans*, both the absolute and the relative yields of TP that lacked a functional PS were increased over those of the PS$^+$ control helper. In spite of this increase in the background, it is clear that the artificial PS in pPMR31 worked almost as well as the wild-type PS in this context. Thus, although the authentic PS competed with the artificial PS very effectively, an arbitrarily chosen double-stranded region by itself could stimulate assembly. The ΔPS constructs pPMR30Δ17 and pPMR48, which were inactive with PS$^+$ helper phage, remained inactive even when the helper phage contained no competing PS.

The filamentous phage Ike shares a common genome organization with f1 (and fd and M13) but has diverged substantially (ca. 50% homology at the coding level) (31). Ike contains a region of dyad symmetry between its gene IV and replication origin that functions as a PS (31). Although there is substantial conservation between the sequences of the two PS regions, the differences between the two led to the prediction of different hairpin structures (Fig. 7). Nonetheless, the Ike PS was very active with f1 helper phage, since pPMR38, the pD6 derivative that contained it, was efficiently packaged with both wild-type and ΔPS helpers (Table 6). The f1 PS must be in the correct orientation with respect to the f1 replication origin to function (9). Similarly, when the DNA fragment containing the Ike PS was present in the

orientation opposite to the f1 replication origin, as in pPMR39, TP were produced at a background level.

DISCUSSION

In infected cells, single-stranded DNA destined for assembly into phage particles is in a complex with pV, a highly cooperative single-stranded DNA-binding protein. For phage to assemble, this protein, which at physiological salt concentrations binds DNA quite tightly (6), must be replaced by the virion structural proteins. This process involves the *cis*-acting PS, the phage structural proteins, and the two helper proteins, products of genes I and IV, which are required for assembly but are not part of the virion (29, 54), as well as the *E. coli* protein thioredoxin (23, 38).

Removal of the PS has drastic effects on assembly. In the absence of a compensating mutation, assembly proceeds at less than 0.1% of the normal rate. This provides strong selection for suppressor mutations, which arise at high frequency and occur, for the most part, in genes IX and I. The experiments presented deal with two questions: (i) what are the essential components of the PS, and (ii) what is the nature of these compensating mutations?

The most obvious feature of the PS is that it can be drawn, and found, as a hairpin. Since gene V protein binds single-stranded DNA much more tightly than double-stranded DNA, this feature suggests that one function of the PS is to provide a region at which gene V protein either will not bind or can easily be displaced. Indeed, Bulsink et al. (6) have calculated that at the protein and salt concentrations found in an infected cell, gene V protein will not bind to the PS hairpin. This can account for the observation that, although the PS is not required for formation of the pV–single-stranded DNA complex (16), when present it is found at an end of this rod-shaped complex (2). Double strandedness alone is not sufficient for PS function, since an artificial PS formed by the head-to-head joining of a restriction fragment cannot complete with a wild-type PS. Nonetheless, the capacity to form a hairpin is important, since the artificial PS works when there is no competing wild-type PS, and since deletions of the authentic PS that by themselves retain function lack PS activity when combined into one construct. The sequence at the tip of the PS is not crucial, since base substitutions and small insertions at the tip can be tolerated and since both the Δ11 deletion and the PS of the related phage Ike, which have different sequences at the tip, are functional. Substantial deletions can be made in the PS without disrupting its function (Fig. 7 and 8). Comparison of the Ike PS with the region of the f1 PS that cannot be deleted shows some sequence homology. In each there is a CGGGT sequence closely followed by a GGTG sequence on the ascending limb of the hairpin and a TGCC sequence on the descending limb (Fig. 7). This last sequence is also found (fortuitously) in the artificial PS, which lacks function. The failure of Δ17 to function could be due to the deletion of two bases from the GGTG sequence shared by the Ike and f1 PS, although it does lack 2 bp from the upper hairpin that are retained in Δ11, and might simply form an insufficiently stable double-stranded structure. Thus a functional packaging signal consists of a combination of a region that can form a hairpin together with specific sequence elements, which, from the deletion analysis, must be located in a relatively small region of the PS (Fig. 7 and 8).

Of the 25 independently isolated phage that had accumulated suppressor mutations, 12 had mutations in gene I (at two sites), and 12 had mutations in gene IX (at three sites). The one mutation in gene VII also altered the promoter for the major coat protein gene. The products of each of these genes are involved in phage assembly. The mutant proteins may have reduced specificity for the PS, enabling them to interact with alternate DNA sequences or structures.

The gene I protein is required for assembly but is not a component of the virion (32, 54). It is an integral membrane protein required for the formation of the increased number of adhesion zones that are found in phage-infected cells (26). These regions, where the inner and outer membrane are joined, are the sites at which assembling phage are extruded (25). It is inferred that the protein is involved in creating the export zone or port through which the phage emerge (26). The N-terminal two-thirds of the protein is located in the cell cytoplasm (19, 20), and it is in this region that the mutations that compensate for inactivation of the PS lie. This suggests that the gene I protein may interact with phage DNA, directly or indirectly. Genetic evidence indicates that the cytoplasmic domain of the protein also interacts with a host protein (thioredoxin) required for filamentous phage assembly (23, 36, 38), but the suppressor mutations that compensate for a PS defect are different from those that suppress thioredoxin missense mutations. In addition, there is a consensus nucleotide-binding site near its N terminus. Thus pI seems to have at least three, not necessarily independent, functions: participating in export pore formation, DNA recognition, and thioredoxin interaction.

The proteins encoded by genes VII and IX are part of the virion (15, 47), and they are required for particle formation (54). The 32-amino-acid gene IX protein and the 33-amino-acid gene VII protein are located at the same end of the phage particle as the PS (53); this is the end that first emerges from the cell, the end at which assembly must be initiated (25). Their proximity in the particle make an interaction between either (or both) of these proteins and the PS a reasonable possibility. pIX is membrane associated (unpublished results), and pVII is thought to be as well. The three different gene IX mutations that compensated for inactivation of the PS were to more hydrophobic amino acids.

The ΔPS phage that have a compensating mutation have a dramatic growth advantage. They are produced at a rate of about 100 phage per min, whereas the rate for ΔPS phage that lack a compensating mutation is less than 0.04 phage per min. This very low rate of production suggests that cells initially infected by suppressorless phage may not assemble phage until a suppressor mutation arises in that cell. Once the mutation occurs, the mutant protein could act in *trans* to promote efficient encapsidation of both mutant and nonmutant single strands.

Two different plasmids, pHV33 and pD6, have been used to evaluate these suppressor mutations. pHV33 single strands exist in small amounts in uninfected *E. coli* and represent less than 0.5% of the single strands present after filamentous phage infection (unpublished results). Thus, encapsidation of pHV33 single strands does not significantly alter the dynamics of phage gene expression and particle assembly. pHV33 TP are normally coencapsidated with a helper phage genome (7; B. Michel, personal communication; Fig. 4). Presumably the PS-containing helper phage genome is located at the leading end of the double-length particle (with the PS at the pVII-pIX end as is normally the case), with the plasmid genome at the lagging end of the particle, incorporated behind an assembling particle that is ultimately to be terminated by the gene III and gene VI proteins. If a wild-type PS is introduced into pHV33, the

plasmid single strands are encapsidated into unit-length particles.

When the helper phage contains a gene I compensating mutation, pHV33 (without the PS) is encapsidated more efficiently and into unit-length particles. Thus an altered gene I protein can initiate the encapsidation of molecules that lack a PS. By contrast, helper phage that contain a gene IX suppressor mutation are unable to initiate pHV33 encapsidation. The I and IX mutant helper phage used in these experiments contained a wild-type PS. Use of helper phages that carried either suppressor mutation but did not have a PS resulted in independent packaging of pHV33. Thus, otherwise assembly-incompetent DNA substrates can be encapsidated if the helper lacks a PS.

The situation with pD6 is quite different and more complex. This plasmid replicates actively after phage infection and competes strongly with the helper for phage-encoded functions. With wild-type helper phage it is encapsidated into unit-length particles, but when the helper is interference resistant (12, 35) about 30% are coencapsidated with helper. Apparently alterations in the dynamics of phage replication, in phage gene expression, and perhaps in the rate of particle assembly can affect encapsidation of molecules that lack a PS. The large amount of single-stranded DNA of pD6 relative to pHV33 (and relative to the PS^+ helper single strands) might account for the ability of pD6 single strands to be singly encapsidated. However, these single strands might also contain a structural feature, missing in pHV33, that allows it to be independently encapsidated even when the helper phage lack a suppressor mutation. For example, pD6 contains the minus-strand replication origin of f1, which consists of two sets of inverted repeats that can form imperfect 14- and 18-bp hairpins. By contrast, the largest potential hairpin identified in a computer search of the pC194 portion of pHV33 was only 12 bp long. Thus the f1 minus-strand hairpins could serve as a weak secondary PS.

By use of the PS and the proteins that appear to interact with it (pI, pIX, and possibly pVII), filamentous phage have evolved an efficient system for both morphogenesis of the final particle and for specifically encapsidating only phage DNA. This specificity is quite stringent with regard to the initiation of assembly, as reflected by the poor growth of phage without a PS. Coencapsidation of two DNA molecules occurs in about 2 to 5% of the particles produced in a wild-type infection (3, 44), and packaging of a second DNA molecule does not seem to require a PS. Thus the phage can carry nonphage DNA, but this would normally occur only in tandem with a phage genome. It seems quite possible that this rather sophisticated transduction scheme could be of value to the phage. Specific mutations in gene I or IX relieve the stringency of the packaging constraint, but molecules with a wild-type PS are still strongly favored. Judging from the results with pHV33, a gene I mutation is more effective than a gene IX mutation in relieving specificity constraints, and it is probable that pI acts before gene IX, since once the IX protein has interacted initiation of packaging has presumably been achieved.

ACKNOWLEDGMENTS

We thank Sarah Thurston, Bettina Niner, and Laurie Proia for excellent technical assistance. We also thank Tracy Ripmaster for sequencing the suppressor mutations. We are very grateful to Benedicte Michel for suggesting that we use pHV33 and for other helpful suggestions. Norton Zinder's criticism of the manuscript was, as always, very valuable.

This work was supported in part by grants from the National Science Foundation and from the National Institutes of Health.

LITERATURE CITED

1. **Adam, M. A., and A. D. Miller.** 1988. Identification of a signal in a murine retrovirus that is sufficient for packaging of nonretroviral RNA into virions. J. Virol. **62**:3802–3806.
2. **Bauer, M., and G. P. Smith.** 1988. Filamentous phage morphogenetic signal sequence and orientation of DNA in the virion and gene-V protein complex. Virology **167**:166–175.
3. **Beaudoin, J., and D. Pratt.** 1974. Antiserum inactivation of electrophoretically purified M13 diploid virions: model for the F-specific filamentous bacteriophages. J. Virol. **13**:466–469.

3a. **Beckett, D., H.-N. Wu, and O. C. Uhlenbeck.** 1988. Roles of operator and non-operator RNA sequences in bacteriophage R17 capsid assembly. J. Mol. Biol. **204**:939–947.

4. **Black, L. W.** 1988. DNA packaging in dsDNA bacteriophages, p. 321–373. *In* Calender (ed.), The bacteriophages, vol. 2. Plenum Publishing Corp., New York.
5. **Boeke, J. D.** 1981. One and two codon insertion mutants of bacteriophage f1. Mol. Gen. Genet. **181**:288–291.
6. **Bulsink, H., B. J. M. Harmsen, and C. W. Hilbers.** 1985. Specificity of the binding of bacteriophage M13 encoded gene-5 protein to DNA and RNA studies by means of fluorescence titrations. J. Biomol. Struct. Dyn. **3**:227–247.
7. **Dagert, M., and S. D. Ehrlich.** 1983. Transitory recombination between plasmid pHV33 and phage M13. EMBO J. **2**:2117–2122.
8. **Deiss, L. P., and N. Frenkel.** 1986. Herpes simplex virus amplicon: cleavage of concatemeric DNA is linked to packaging and involves amplification of the terminally reiterated *a* sequence. J. Virol. **57**:933–941.
9. **Dotto, G. P., V. Enea, and N. D. Zinder.** 1981. Functional analysis of bacteriophage f1 intergenic region. Virology **114**: 463–473.
10. **Dotto, G. P., and N. D. Zinder.** 1983. The morphogenetic signal of bacteriophage f1. Virology **130**:252–256.
11. **Eggen, K., and D. Nathans.** 1969. Regulation of protein synthesis directed by coliphage MS2 RNA. II. *In vitro* repression by phage coat protein. J. Mol. Biol. **39**:293–305.
12. **Enea, V., and N. D. Zinder.** 1982. Interference resistant mutants of phage f1. Virology **122**:222–226.
13. **Fidanian, H. M., and D. S. Ray.** 1972. Replication of bacteriophage M13. VII. Requirement of the gene 2 protein for the accumulation of a specific RFII species. J. Mol. Biol. **72**:51–63.
14. **Fulford, W. D., and P. Model.** 1984. Gene X of bacteriophage f1 is required for phage DNA synthesis. J. Mol. Biol. **178**:137–153.
15. **Grant, R. A., T. C. Lin, W. Konigsberg, and R. E. Webster.** 1981. Structure of the filamentous bacteriophage f1. Location of the A, C and D minor coat proteins. J. Biol. Chem. **256**:539–546.
16. **Grant, R. A., and R. E. Webster.** 1984. The bacteriophage f1 morphogenetic signal and the gene V protein/phage single-stranded DNA complex. Virology **133**:329–340.
17. **Gros, M. R., H. te Riele, and S. D. Ehrlich.** 1987. Rolling circle replication of single-stranded DNA plasmid pC194. EMBO J. **6**:3863–3869.
18. **Hill, D. F., and G. B. Petersen.** 1982. Nucleotide sequence of bacteriophage f1 DNA. J. Virol. **44**:32–46.
19. **Horabin, J. I., and R. E. Webster.** 1986. Morphogenesis of f1 filamentous bacteriophage: increased expression of gene I inhibits bacterial growth. J. Mol. Biol. **188**:403–413.
20. **Horabin, J. I., and R. E. Webster.** 1988. An amino acid sequence which directs membrane insertion causes loss of membrane potential. J. Biol. Chem. **263**:11575–11583.
21. **Huang, C.-C., and J. E. Hearst.** 1981. Fine mapping of secondary structures of fd phage DNA in the region of the replication origin. Nucleic Acids Res. **9**:5587–5599.
22. **Ikoku, A. S., and J. E. Hearst.** 1981. Identification of a structural hairpin in the filamentous chimeric phage M13*Gori*1. J. Mol. Biol. **151**:245–259.
23. **Lim, C. J., B. Haller, and J. A. Fuchs.** 1985. Thioredoxin is the bacterial protein encoded by *fip* that is required for filamentous bacteriophage f1 assembly. J. Bacteriol. **161**:799–802.

24. **Ling, C. M., P. P. Hung, and L. R. Overby.** 1970. Independent assembly of Qβ and MS2 phages in doubly infected *Escherichia coli*. Virology **40**:920–929.
25. **Lopez, J., and R. E. Webster.** 1983. Morphogenesis of filamentous bacteriophage f1: orientation of extrusion and production of polyphage. Virology **127**:177–193.
26. **Lopez, J., and R. E. Webster.** 1985. Assembly site of bacteriophage f1 corresponds to adhesion zones between the inner and outer membranes of the host cell. J. Bacteriol. **163**:1270–1274.
27. **Maniatis, T., E. F. Fritsch, and J. Sambrook.** 1982. Molecular cloning: a laboratory manual. Cold Spring Harbor Laboratory, Cold Spring Harbor, N.Y.
28. **Mann, R., and D. Baltimore.** 1985. Varying the position of a retrovirus packaging sequence results in the encapsidation of both unspliced and spliced RNAs. J. Virol. **54**:401–407.
29. **Model, P., and M. Russel.** 1988. Filamentous bacteriophage, p. 375–456. *In* R. Calender (ed.), The bacteriophages, vol. 2. Plenum Publishing Corp., New York.
30. **Moses, P. B., J. D. Boeke, K. Horiuchi, and N. D. Zinder.** 1980. Restructuring the bacteriophage f1 genome: expression of gene VIII in the intergenic space. Virology **104**:267–278.
31. **Peeters, B. P. H., R. M. Peters, J. G. G. Schoenmakers, and R. N. H. Konings.** 1985. Nucleotide sequence and genetic organization of the genome of the N-specific filamentous bacteriophage IKe: comparison with the genome of the F-specific filamentous phage M13, fd, and f1. J. Mol. Biol. **181**:27–39.
32. **Pratt, D., H. Tzagoloff, and W. S. Erdahl.** 1966. Conditional lethal mutants of the small filamentous coliphage M13. I. Isolation, complementation, cell killing, time of cistron action. Virology **30**:397–410.
33. **Pugatsch, T., and D. W. Stacey.** 1983. Identification of a sequence likely to be required for avian retroviral packaging. Virology **128**:505–511.
34. **Rasched, I., and E. Oberer.** 1986. Ff coliphages: structural and functional relationships. Microbiol. Rev. **50**:401–427.
35. **Russel, M., S. Kidd, and M. R. Kelley.** 1986. An improved filamentous helper phage for generating single-stranded plasmid DNA. Gene **45**:333–338.
36. **Russel, M., and P. Model.** 1983. A bacterial gene, *fip*, required for filamentous bacteriophage f1 assembly. J. Bacteriol. **154**: 1064–1076.
37. **Russel, M., and P. Model.** 1985. Direct cloning of the *trxB* gene that encodes thioredoxin reductase. J. Bacteriol. **163**:238–242.
38. **Russel, M., and P. Model.** 1985. Thioredoxin is required for filamentous phage assembly. Proc. Natl. Acad. Sci. USA **82**: 29–33.
39. **Russel, M., and P. Model.** 1986. The role of thioredoxin in filamentous phage assembly. Construction, isolation, and characterization of mutant thioredoxins. J. Biol. Chem. **261**:14997–15005.
40. **Sanger, F., S. Nicklen, and A. R. Coulson.** 1977. DNA sequencing with chain terminating inhibitors. Proc. Natl. Acad. Sci. USA **74**:5463–5467.
41. **Schaller, H.** 1979. The intergenic region and the origins for filamentous phage DNA replication. Cold Spring Harbor Symp. Quant. Biol. **43**:401–408.
42. **Schaller, H., E. Beck, and M. Takanami.** 1978. Sequence and regulatory signals of the filamentous phage genome. p. 139–163 *In* D. T. Denhardt, D. Dressler, and D. S. Ray (ed.), The single-stranded DNA phages. Cold Spring Harbor Laboratory, Cold Spring Harbor, N.Y.
43. **Schaller, H., H. Voss, and S. Gucker.** 1969. Structure of the DNA of bacteriophage fd. II. Isolation and characterization of a DNA fraction with double strand-like properties. J. Mol. Biol. **44**:445–458.
44. **Scott, J. R., and N. D. Zinder.** 1967. Heterozygotes of phage f1, p. 212–218. *In* J. S. Colter and W. Paranchych (ed.), The molecular biology of viruses. Academic Press, Inc., New York.
45. **Shen, C. K. J., A. Ikoku, and J. E. Hearst.** 1979. Specific DNA orientation in the filamentous bacteriophage fd as probed by psoralen crosslinking and electron-microscopy. J. Mol. Biol. **127**:163–175.
46. **Shen, C. K. J., and J. E. Hearst.** 1976. Psoralen-crosslinked secondary structure map of single-stranded virus DNA. Proc. Natl. Acad. Sci. USA **73**:2649–2653.
47. **Simons, G. F. M., R. N. H. Konings, and J. G. G. Schoenmakers.** 1981. Genes VI, VII, and IX of phage M13 code for minor capsid proteins of the virion. Proc. Natl. Acad. Sci. USA **78**:4194–4198.
48. **Sleat, D. E., P. C. Turner, J. T. Finch, P. J. G. Butler, and T. M. A. Wilson.** 1986. Packaging of recombinant RNA molecules into pseudovirus particles directed by the origin-of-assembly sequence from tobacco mosaic virus RNA. Virology **155**:299–308.
49. **te Riele, H., B. Michel, and S. D. Ehrlich.** 1986. Are single-stranded circles intermediates in plasmid DNA replication? EMBO J. **5**:631–637.
50. **te Riele, H., B. Michel, and S. D. Ehrlich.** 1986. Single-stranded plasmid DNA in *Bacillus subtilis* and *Staphylococcus aureus*. Proc. Natl. Acad. Sci. USA **83**:2541–2545.
51. **Turner, D. R., and P. J. G. Butler.** 1986. Essential features of the assembly origin of tobacco mosaic virus RNA as studied by directed mutagenesis. Nucleic Acids Res. **14**:9229–9242.
52. **Turner, D. R., L. E. Joyce, and P. J. G. Butler.** 1988. The tobacco mosaic virus assembly origin RNA: functional characteristics defined by directed mutagenesis. J. Mol. Biol. **203**: 531–547.
53. **Webster, R. E., R. A. Grant, and L. A. W. Hamilton.** 1981. Orientation of the DNA in the filamentous bacteriophage f1. J. Mol. Biol. **152**:357–374.
54. **Webster, R. E., and J. Lopez.** 1985. Structure and assembly of the class I filamentous bacteriophage, p. 235–268. *In* S. Casjens (ed.), Virus structure and assembly. Jones and Bartlett, Boston.
55. **Zimmern, D., and P. J. G. Butler.** 1977. The isolation of tobacco mosaic virus RNA fragments containing the origin for viral assembly. Cell **11**:455–462.